Maleated Ethylene-Propylene Random Copolymers: Determination of the Microstructure and Association Level by Fluorescence Spectroscopy

Veena Vangani, Jillian Drage, Junaid Mehta, Anna K. Mathew, and Jean Duhamel*

Institute of Polymer Research, Department of Biochemistry and Chemistry, University of Waterloo, Waterloo, ON N2L 3G1, Canada

Received: October 26, 2000; In Final Form: March 7, 2001

A maleated ethylene-propylene (EP) random copolymer was labeled with the fluorescent dye 1-pyrenebutanoicacid hydrazide to yield EP−Py. Fluorescence spectroscopy was used to determine the microstructure of EP−Py (i.e., the distribution of the pendants along the chain) in THF where little association is expected to occur between the polar pendants. In hexane, an apolar solvent, associations take place between the polar pendants and the association level of EP−Py (i.e., fractions of pendants, which are associated and unassociated) was estimated by analyzing quantitatively both the monomer and the excimer fluorescence decays. The ability of pyrene to form an excimer was used to carry out this study. The excimer formation process was monitored by using a combination of two models, namely the *sequential* model and the *blob* model. Both monomer and excimer decays were analyzed in order to completely describe the distribution of pyrene groups. It was found that 70% of all pyrene groups are located at small distances from one another and form excimer readily. In apolar hexane, 87% of all pyrene groups are involved into loose pyrene aggregates, held together via polar interactions between the succinic anhydride groups.

Introduction

Peculiar viscoelastic properties are often encountered with polymeric solutions made with a polymer onto which insoluble units have been attached.[1] These properties are the result of polymer aggregates, which are formed via intermolecular associations occurring between the insoluble moieties of the modified polymer. The polymer aggregates are large entities which usually result in solutions having large viscosities. However, the associations between insoluble moieties are not permanent since no chemical bond is formed. Consequently, these associations collapse when they are subject to some stress such as shear and the polymer solution thins. These polymers have been coined associative polymers (AP), and they have found numerous practical applications notably in the coating industry as associative thickeners,[2] but also as drag reducing agents in pipelines, oil recovery agents, or viscosity modifiers in oils.[1]

Since the viscoelastic properties of AP solutions arise from the associations between insoluble pendants, the association level of the insoluble moieties (i.e., how many moieties are associated versus unassociated) is an important parameter toward the complete characterization of such a system. This is because an AP's association level is related to its associative strength. Unfortunately, APs association level is very rarely reported. Few techniques can provide this information in a direct manner. The analysis of rheology measurements proceeds via models, which determine the locations of the insoluble pendants in the polymeric network.[3] The insoluble pendants distribute themselves into either close micelles (where the insoluble moieties of a single chain are pooled together inside an insoluble aggregate), open micelles (where the insoluble aggregates are made of the insoluble moieties of different AP chains), or dangling pendants. The distribution of the insoluble pendants into these various entities is a consequence of the distribution of chain states in the AP network. The dynamic rheology data are interpreted by assuming that each entity yields a different viscoelastic response. NMR experiments can also distinguish between an AP's associated and unassociated pendants. The unassociated pendants exhibit a chemical shift, which changes upon association. By integrating the signal of the associated and unassociated pendants, it is possible to quantify their level of association.[4] In this report, we propose to use the ability of the dye pyrene to form excimer in order to determine the level of association of an AP by fluorescence spectroscopy.

The pyrene excimer is an excited complex, which is the result of the encounter between a ground-state pyrene and a pyrene excited by photon absorption.[5] Whereas the excited pyrene monomer exhibits sharp emission peaks around 370−390 nm, the excimer emits a broad structureless fluorescence centered around 480 nm. In this work, the dye pyrene is attached onto an AP's associating pendants. Because the time required to form an excimer depends on the distance spanning two pyrene groups, it takes more time to form an excimer when the pyrene groups are attached at remote positions on the polymer backbone than when they are located close to one another. We take advantage of this feature to determine the fraction of pyrene groups which are forming excimer on a fast time scale (decay times shorter than about 10 ns) and the fraction of pyrene groups which are forming excimer by diffusion on a slower time scale. In so doing we can distinguish between domains in the AP coil which contain a high concentration of associating pendants and where excimer formation is fast and domains of the AP coil where the associating pendants are displayed as single units along the AP backbone.

The system, which we propose to investigate, is an ethylene-propylene (EP) copolymer. EP copolymers are used in the oil-additive industry as viscosity modifiers.[6] Their purpose as motor-oil additives is 2-fold. First their coil size undergoes large

* To whom correspondence should be addressed.

10.1021/jp0039722 CCC: $20.00
Published on Web 05/04/2001

SCHEME 1: Representation of EP−Py[a]

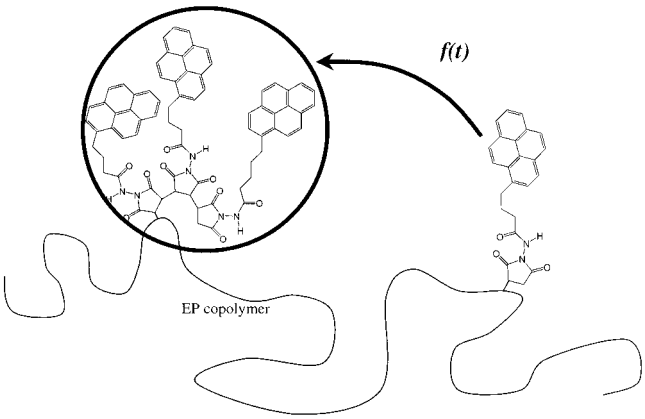

[a] The maleated EP copolymer was labeled with PHZ. PHZ attaches onto either single succinic anhydride units or oligoMA. Labeling of the oligoMA yields a loose pyrene aggregate, which is indicated by the solid circle. the function $f(t)$ describes the rate of encounter between pyrene groups randomly distributed along the polymer backbone.

variations with temperature.[7] At low temperatures, long polyethylene stretches of EP copolymers in oil crystallize, which reduces the overall dimensions of the polymer coil and lowers the solution viscosity. At high temperatures, no crystallite remains, and the coil expands increasing the viscosity. Consequently, the addition of an EP copolymer to a motor-oil offsets the decrease in viscosity which is normally observed when a fluid is heated and the mixture exhibits improved lubricating properties. The second purpose for using EP copolymers as motor oil additives is because these unreactive polymers can be easily functionalized by grafting them with maleic anhydride (MA). The maleated copolymer is further reacted with amino-compounds to yield an oil-soluble polymer with polar groups randomly distributed along its backbone. In apolar oil, the polar groups associate.[8] This type of oil-soluble associating polymer is used to stabilize polar particulate matter, which is generated during the normal working of an engine. By preventing the formation of soot, this oil additive ensures that the motor oil works longer. In this study, the amino-compound 1-pyrenebutanoicacid hydrazide (PHZ) is reacted with the maleated EP copolymer to yield the pyrene-labeled EP copolymer (EP−Py), whose structure is described in Scheme 1.

The most remarkable feature of maleated EP copolymers is their utter lack of definition. Maleated polyolefins are usually polydisperse in length; the succinic anhydride pendants are randomly located along the backbone; oligoMA as well as single MA units can attach onto the polyolefin backbone.[9] A priori, such lack of definition should forbid any quantitative fluorescence analysis based on excimer formation, because the excimer formation process depends strongly on the distance between dyes, so that the distributions of (1) polymer chain lengths and (2) distances between dyes both induce a quasi infinite distribution of excimer formation rates.[10,11] An added complication arises from the use of the dye pyrene. Polar associations occurring between the succinic anhydride groups in apolar solvents induce the formation of pyrene ground-state (GS) dimers, which further complicates the system, since one additional fluorescent species is present in solution.[12] These complications are rather unfortunate because they make it difficult to determine quantitatively the number of pyrene-labeled pendants, which are associated or unassociated, a critical information for the complete characterization of an AP.

Over the recent years, my research group has shown that a complete assignment of the pyrene-labeled pendants requires analyzing the pyrene monomer and excimer fluorescence decays. To this effect several tools were developed in order to characterize the behavior of better-defined AP systems by fluorescence. The association process between pyrene groups attached at well determined positions of a poly(ethylene oxide) was characterized in water by using a *sequential* model.[13] In the *sequential* model, pyrene groups diffuse toward each other to form a loose pyrene aggregate held together by hydrophobic forces in water. Then the pyrene moieties rearrange themselves on a fast time scale in order to form the pyrene excimer. The *sequential* model was also applied to monitor the process of excimer formation in hexane for a poly(isobutylene) onto which a MA unit has been attached at a single end.[14] The *sequential* model is based on the concept of *capture* radius proposed originally by Char et al.[15] With respect to the distribution of excimer formation rates, we have showed that the process of excimer formation occurring between pyrene groups randomly attached along a polymer backbone can be successfully handled by using a *blob* model.[11] With the *blob* model approach, the polymer coil is divided into *blobs* among which the pyrene groups are randomly distributed according to a Poisson distribution. As any *blob*-based approach, the *blob* model shifts the focus of interest from the whole polymer chain down to a single *blob*. A long polymer chain is made of many *blobs*, whereas a shorter one is made of fewer similar *blobs*. Consequently the mathematical bases of the *blob* model handle any problem arising from the distributions of chain lengths and random positions of the pyrene groups. The fluorescence decays of the excited pyrene monomer can be fitted according to a Tachiya-Infelta-Gratzel-Thomas type equation,[16] which uses three parameters.[11] They are the rate constant k_{diff} of excimer formation inside a *blob* containing one excited pyrene and one GS pyrene, the rate constant at which pyrene groups exchange from *blob* to *blob* given by the product of the exchange rate constant and the blob concentration inside the polymer coil k_e[blob], and the average number of pyrene groups per *blob* $\langle n \rangle$.

The purpose of this work is to determine quantitatively by fluorescence the fractions of an AP's associating pendants, which are associated and unassociated. Depending on whether the fraction of associated pendants (f_{AP}) is close to 1.0 or 0.0, the AP can be considered to exhibit good or poor associative strength, respectively. However, such analysis requires knowledge of the distribution of associating pendants along the AP backbone. Two extreme cases are shown in Scheme 2. In the upper panel, all pendants are well spread out along the chain. The switch from a solvent, which does not promote polar associations, to an association promoting solvent yields a clear-cut picture where f_{AP} goes from 0.0 to 1.0. Unfortunately this idealized illustration is not often encountered in real life systems. Since the associating pendants are usually introduced randomly into the polymer backbone, the chance is that some associating pendants will be present close to one another. This is even more so for the maleated EP copolymer under study, for numerous reports have shown that MA grafting leads to the formation of oligoMA attached onto the backbone.[9] The worse possible case is shown in the lower panel of Scheme 2, where f_{AP} equals 1.0, regardless of the solvent quality toward the insoluble pendants. In this example, the distribution of the associating pendants precludes any conclusion regarding the AP's associative strength. It becomes clear from the considerations discussed above that knowledge of an AP's microstructure is necessary prior to investigating the AP's associative strength.

Pyrene is by far the dye most used to study polymeric systems by fluorescence.[12] Improving our ability to correlate the behavior

SCHEME 2: Importance of the Microstructure of a Modified Polymer When Determining Its Association Level[a]

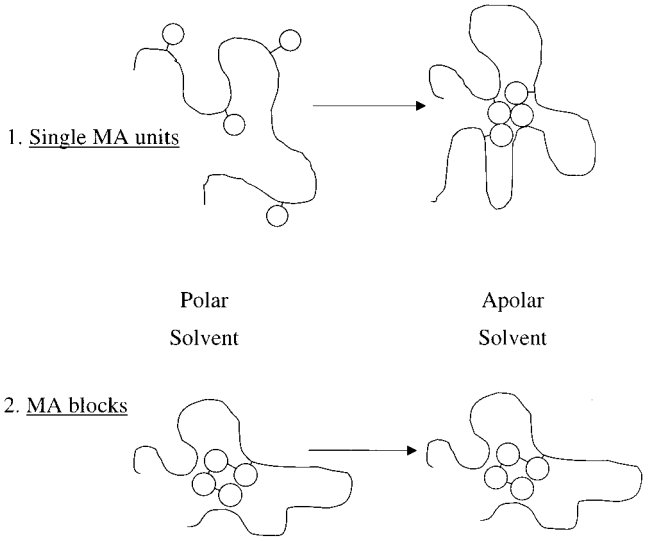

[a] The circle represent MA units.

of the dye with the properties of the polymer, which it is bound to, would certainly open new venues of research. In this report, both the *sequential* model and the *blob* model are combined into basic models aimed at determining the fractions of associating pendants, which are either free or involved into aggregates. This combined approach, which is applied to the monomer and the excimer decays of EP−Py in tetrahydrofuran (THF) and hexane, yields the microstructure and the association level of this polymer. To the best of our knowledge, it is the first time that the monomer and excimer decays of such a complicated pyrene labeled AP system are analyzed in a quantitative manner toward retrieving this type of information.

Experimental Section

All solvents, materials, syntheses, techniques and instruments were described in an earlier report.[17]

Polymer Characterization. The EP random copolymer grafted with maleic anhydride and labeled with pyrene (EP−Py) was a generous gift from Ethyl Corporation.[17] This polymer contained 60 mol % of ethylene and 9×10^{-5} mol of pyrene/gram of EP copolymer. EP−Py has an estimated M_n of 25 000 and PDI = 1.6, based on a calibration of the SEC system using polystyrene standards.

Fluorescence Decay Analysis. A function $g(t)$ was assumed for the fluorescence decays. It was convoluted with the instrument response function $L(t)$ to fit the experimental decay $G(t)$[18]

$$G(t) = L(t) \otimes g(t) \tag{1}$$

where the symbol ⊗ indicates the convolution performed between the experimental instrument function and the fitting function $g(t)$. Two methods were used to optimize the fit of the fluorescence decays. The first method was based on the Marquardt−Levenberg algorithm.[19a] The function $g(t)$ was either a sum of exponentials with an expression given in eq 2 where the number of exponentials n is varied from 1 to 4, or the more complicated eqs 4a and 10a, which are presented in the Results and Discussion section and whose derivations are given in the Appendices A and B. The index X in eq 2 is either M or E for the monomer or the excimer, respectively. Equations 4a and 10a involve an infinite series, which was calculated up to the 11th term in our analysis programs. According to the experimental parameters that we retrieved from our analysis, the contribution of the higher terms is negligible. The parameters of $g(t)$ were retrieved by using a least-squares curve fitting program based on the Marquardt−Levenberg algorithm.[19a]

$$g(t) = \sum_{\substack{i=1 \\ X=M,E}}^{i=n} A_{Xi} e^{-t/\tau_{Xi}} \tag{2}$$

Typical initial guesses for fitting the monomer decays with eqs 4a and 10a were $k_{agg} = 20 \times 10^7\ s^{-1}$, $<n> = 1.5$, $k_{diff} = 2 \times 10^7\ s^{-1}$, and $k_e[blob] = 0.3 \times 10^7\ s^{-1}$. Changing these initial guesses by ±50% led to the same solution.

The second method was applied to fit the excimer fluorescence decays with eqs 4b and 10b. Fixing the parameters k_{agg}, A_2, A_3, A_4, and τ_{E2} in eqs 4b and 10b transforms these two equations into a linear sum of four functions. A General Linear Least Squares routine was used to fit the excimer fluorescence decays.[19b] The χ^2 parameter was optimized by applying a Golden Section Search to the lifetime τ_{E1}.[19c] Due to the nature of the General Linear Least-Squares routine, no initial guesses were needed to initialize the fitting procedure.

For all fluorescence decays, the quality of the fits was assessed from the χ^2 parameter ($\chi^2 < 1.2$ for a good fit) and the random distribution of the residuals and of the autocorrelation function.

Simulation of Fluorescence Decays. The analysis of the fluorescence decays required numerous parameters (seven for the pyrene monomer and 11 for the excimer). It was thus important to estimate the level of accuracy of our analysis method. To this end, fluorescence decays of the monomer and the excimer were simulated with 10 different Poisson noise patterns using the parameters retrieved from a given decay.[20] The results from the analysis of the 10 simulated decays were averaged and their standard deviation was calculated. For all but two parameters (k_{agg} and k_{diff}, which are defined later in the text and are retrieved with less than ±15% uncertainty), less than ±10% uncertainty was achieved using our procedure. One example of each type of analysis is given in Tables 2a,b and 4a,b.

Results and Discussion

To thoroughly characterize EP−Py, its microstructure must be determined. This task is carried out in the following section. The EP−Py association level is then determined in the later section.

Microstructure of the Maleated EP Copolymer. The expected microstructure of EP−Py is shown in Scheme 1. Since pyrene is attached onto the MA pendants, the presence of oligoMA creates pyrene-rich domains, which promote the formation of pyrene GS dimers, even in a solvent, which does not promote associations such as THF. The presence of pyrene GS dimers can be established by carrying out steady-state excitation measurements. In an earlier report, we had shown that a spectral shift was clearly visible between the excitation spectra of EP−Py in hexane (Figure 2B in Vangani et al.[17]) acquired with an emission wavelength fixed at either 377 nm (for the pyrene monomer) or 500 nm (for the pyrene excimer). The spectral shift was strongly reduced but still visible in THF (Figure 2A in Vangani et al.[17]) indicating that much less pyrene GS dimers were present in THF. This was an expected result because THF is more polar than hexane and thus does not

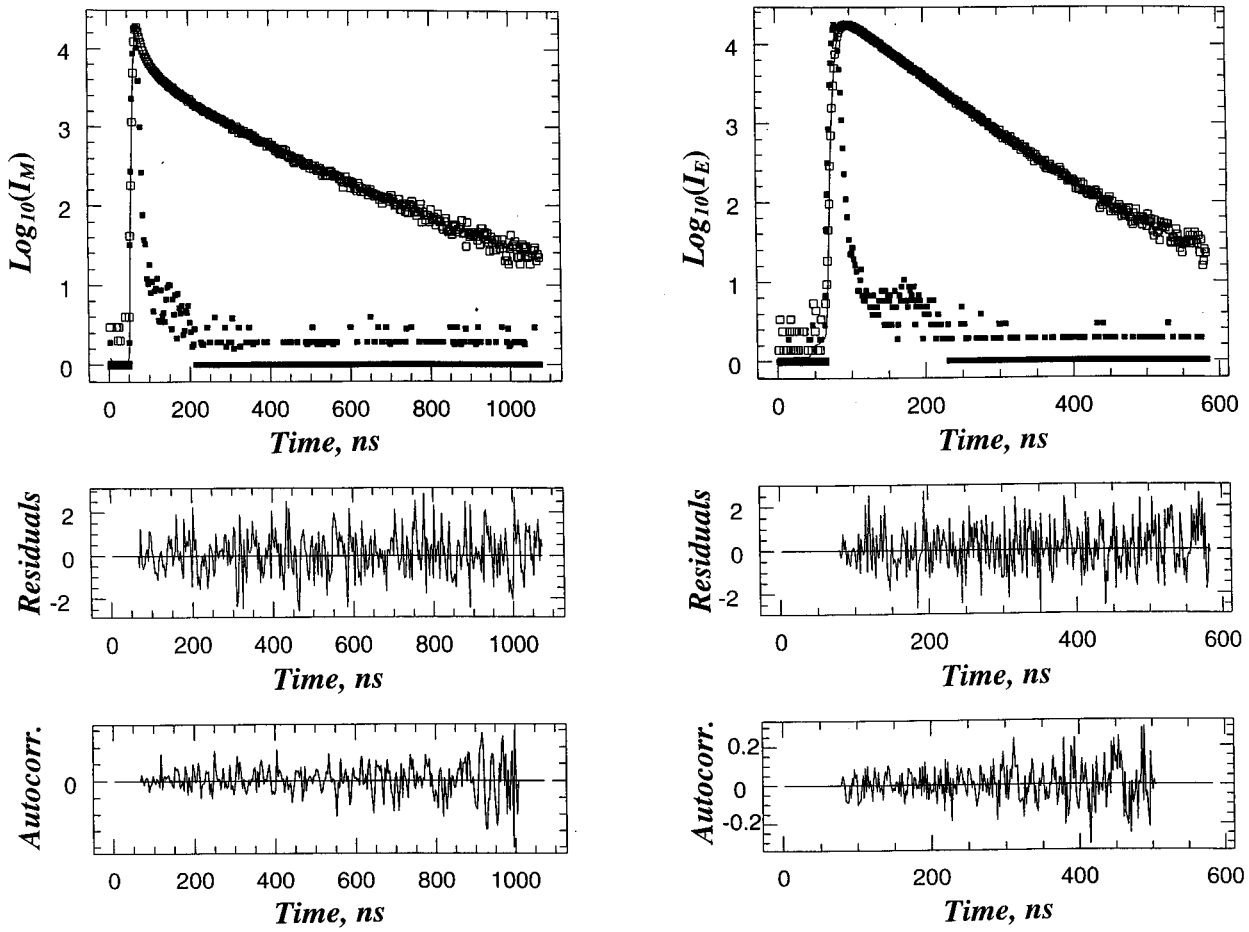

Figure 1. Fluorescence decays of EP−Py monomer (λ_{ex} = 344 nm, λ_{em} = 377 nm) and excimer (λ_{ex} = 344 nm, λ_{em} = 520 nm) with a polymer concentration of 0.25 g/L in THF. The monomer and excimer decays were fitted with eqs 4a and 4b, respectively.

promote the polar associations between the grafted MA groups. However the presence of a slight shift observed in THF does indicate that some residual association between pyrene groups subsists, even in this more polar solvent.

Fluorescence excimer decays can also indicate the presence of pyrene GS dimers. Monomer and excimer decays were acquired for EP−Py in THF. A typical example of such decays is shown in Figure 1. All decays were first fitted with a sum of exponentials. Table 1 lists the preexponential factors and decaytimes obtained for EP−Py in THF at different polymer concentrations. Three to four exponentials were required in order to fit the pyrene monomer decays. The longest decaytime was fixed to equal the lifetime of a single PHZ attached onto a maleated polymer in THF (τ_M = 210 ns)[14] and the excimer decays were fitted with three exponentials. Since the monomer and excimer decays could not be fitted with two exponentials, the classic Birks' scheme used to study the kinetics of excimer formation was not applicable in this case.[5] Although the kinetics exhibited in the monomer and excimer decays are complicated, some general features can be observed. All the excimer decays yield a ratio $a_{E1}/(a_{E2} + a_{E3})$ more positive than −1.0, which indicates the presence of pyrene GS dimers.[17,21] The excimer decays exhibit a short rise time, which is given by the first decaytime τ_{E1} and equals 10.5 ± 1.0 ns. It is paralleled by a short decaytime τ_{M1} in the monomer decays. The short decaytime τ_{M1} in the monomer decays and the short rise time τ_{E1} in the excimer decays indicate that some excimers are formed on a fast time scale. Rapid excimer formation would be expected inside a loose pyrene aggregate, where pyrene moieties are held within a small restricted volume via oligoMA or single MA molecules attached on nearby polymeric units. Pyrene ground-state dimers can only be found inside the loose pyrene aggregates, but not all loose pyrene aggregates contain ground-state pyrene dimers. For instance, Scheme 1 represents a loose pyrene aggregate where no pyrene ground-state dimer is present. The second decaytime τ_{E2} of the excimer equals 60 ± 1 ns which is a reasonable value for the pyrene excimer lifetime.[5] The contribution of the third exponential in the excimer decays was very small but was necessary to obtain good fits. The third decaytime τ_{E3} was obtained with little accuracy, but it was larger than 100 ns. The decaytimes τ_{M2} and τ_{M3} in the monomer decays are expected to represent a slower excimer formation process such as the one due to diffusional encounters.

To analyze these measurements in a more quantitative manner, reaction Scheme 3 is introduced to account for all the decay features discussed in the previous paragraph. Loose pyrene aggregates (Py_{agg}) as well as single pyrenes (Py_{diff}) are distributed randomly along the polymer backbone. Loose pyrene aggregates result from the presence of either oligoMA or single MA molecules, which are grafted onto neighboring polymer units. Excimer formation is assumed to arise from exciting either a pyrene inside a loose pyrene aggregate or a single pyrene on the polymer backbone. Within a loose pyrene aggregate, excimer formation occurs on a fast time scale with a rate constant k_{agg}. A single excited pyrene (Py^*_{diff}) forms excimer via diffusional encounter with either a single GS pyrene or a loose pyrene aggregate. Both Py_{agg} and Py_{diff} species act as a quencher for Py^*_{diff} and are referred to as Q in the following discussion.

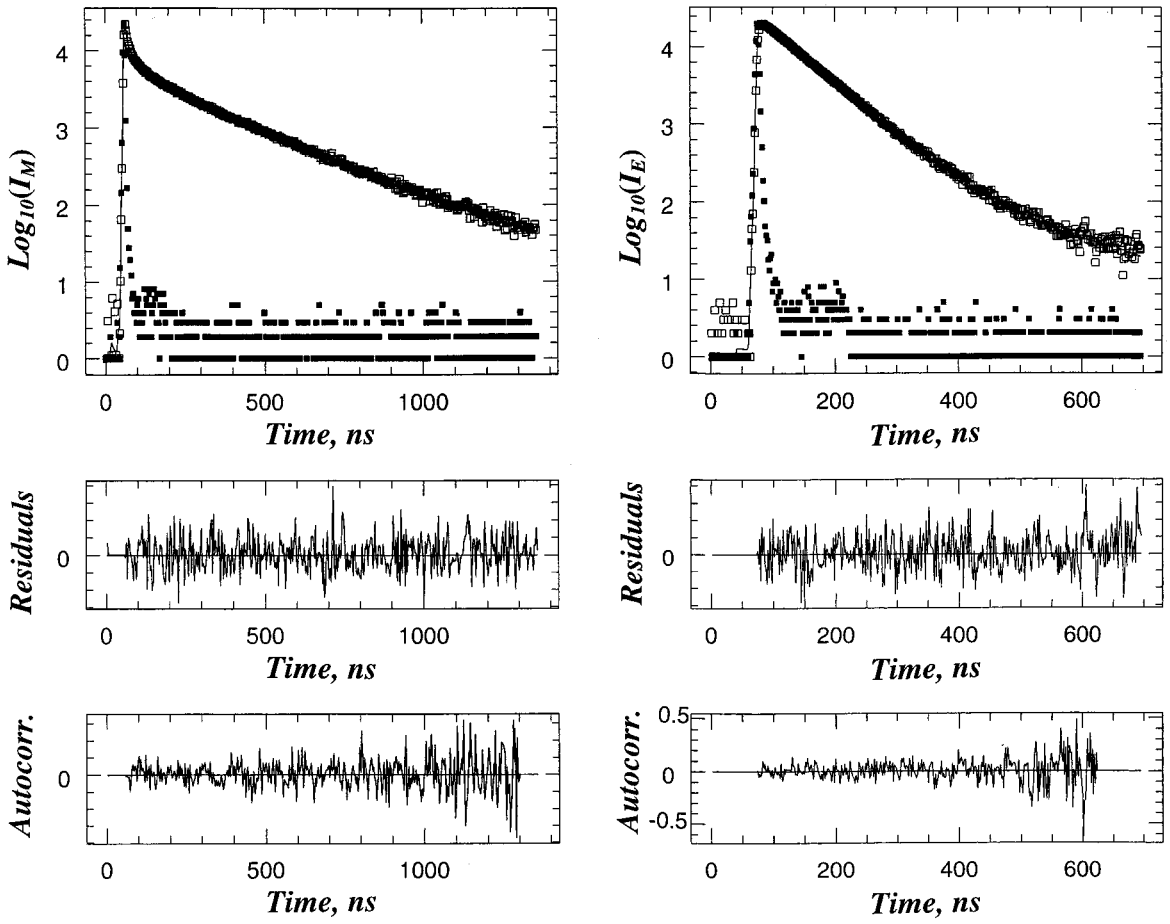

Figure 2. Fluorescence decays of EP−Py monomer (λ_{ex} = 344 nm, λ_{em} = 377 nm) and excimer (λ_{ex} = 344 nm, λ_{em} = 520 nm) with a polymer concentration of 0.04 g/L in hexane. The monomer and excimer decays were fitted with eqs 10a and 10b, respectively.

TABLE 1

(a) Parameters Retrieved from the Tri- or Four-Exponential Fit of the Pyrene Monomer Fluorescence Decays of EP−Py in THF (λ_{ex} = 344 nm, λ_{em} = 377 em)

[Poly] (g/L)	a_{M1}	τ_{M1} (ns)	a_{M2}	τ_{M2} (ns)	a_{M3}	τ_{M3} (ns)	a_{M4}	τ_{M4} (ns)	χ^2
0.38			0.68	13	0.21	74	0.11	210	1.29
0.25	0.60	7.6	0.24	36	0.08	121	0.08	210	1.12
0.13	0.52	6.7	0.27	29	0.12	108	0.09	210	1.07
0.07	0.56	5.6	0.24	22	0.12	82	0.08	210	1.15

(b) Parameters Retrieved from the Tri-Exponential Fit of the Pyrene Excimer Fluorescence Decays of EP−Py in THF (λ_{ex} = 344 nm, λ_{em} = 520 nm)

[Poly] (g/L)	a_{E1}	τ_{E1} (ns)	a_{E2}	τ_{E2} (ns)	a_{E3}	τ_{E3} (ns)	χ^2
0.38	−0.62	9.8	1.00	61	<0.01	228	1.13
0.25	−0.54	10.4	1.00	60	0.02	103	1.22
0.13	−0.52	10.0	1.00	60	<0.01	119	1.29
0.07	−0.49	11.9	1.00	59	0.01	144	1.07

Because Py_{agg} and Py_{diff} are randomly distributed along the polymer backbone, a complicated function $f(t)$ describes the rate at which an excimer (E1*) is formed via diffusional encounters between Py^*_{diff} and Q. $f(t)$ is introduced to account for the distribution of rate constants for excimer formation. The excimer E1* can also be formed within Py^*_{agg} with a rate constant k_{agg}. Beside the excimer E1*, which fluoresces with a typical excimer lifetime of about 60 ns, the presence of residual long-lived excited pyrene dimers (E2*) could be detected and needed to be accounted for. The reason for introducing E2* is discussed later on in the article. Also some excited pyrenes are not being quenched because they are either too far from a quencher species or because the polymer chain displays a single dye. These pyrene groups are referred to as Py^*_{free}. Scheme 3 does not account for the dissociation of the pyrene excimer, which is known to exhibit a small rate constant at room temperature.[5,14] The time-dependent behaviors of Py^*_{diff}, Py^*_{agg}, Py^*_{free}, E1*, and E2* are described in the five following differential equations:

$$\frac{d[Py^*_{agg}]}{dt} = -\left(k_{agg} + \frac{1}{\tau_M}\right)[Py^*_{agg}] \quad (3a)$$

$$\frac{d[Py^*_{free}]}{dt} = -\frac{1}{\tau_M}[Py^*_{free}] \quad (3b)$$

$$\frac{d[Py^*_{diff}]}{dt} = -f(t) - \frac{1}{\tau_M}[Py^*_{diff}] \quad (3c)$$

$$\frac{d[E1^*]}{dt} = k_{agg}[Py^*_{agg}] + f(t) - \frac{1}{\tau_{E1}}[E1^*] \quad (3d)$$

$$\frac{d[E2^*]}{dt} = -\frac{1}{\tau_{E2}}[E2^*] \quad (3e)$$

The time-dependent behavior of the pyrene monomer and excimer is obtained by integrating eqs 3a−e. The mathematical treatment is given in Appendix A. The only difficulty resides in determining an expression for the function $f(t)$. This is accomplished by applying the *blob* model to characterize the quenching process of Py^*_{diff} by Q.[11] The final equations for the

TABLE 2

(a) Parameters Retrieved from Fitting the Pyrene Monomer Fluorescence Decays of EP−Py in THF with eq 4a

[Poly] (g/L)	f_{Magg}	f_{Mdiff}	f_{Mfree}	k_{agg} (10^7 s^{-1})	$\langle n \rangle$	k_{diff} (10^7 s^{-1})	k_e[blob] (10^7 s^{-1})	χ^2
0.38	0.57	0.39	0.05	12.0	1.71	1.1	0.1	1.01
0.25	0.45	0.47	0.07	15.0	1.80	1.8	0.3	1.07
0.25[a]	(0.47) ± 0.04	(0.46) ± 0.04	(0.07) ± 0.00	(14.9) ± 1.7	(1.81) ± 0.04	(1.7) ± 0.2	(0.3) ± 0.0	(0.97) ± 0.03
0.13	0.57	0.39	0.05	13.6	1.74	1.2	0.1	1.07
0.07	0.55	0.39	0.07	16.4	1.86	1.7	0.3	1.16

(b) Parameters Retrieved from Fitting the Pyrene Excimer Fluorescence Decays of EP−Py in THF with eq 4b

[Poly] (g/L)	f_{Eagg}	f_{Ediff}	f_{EE1}	f_{EE2}	τ_{E1} (ns)	χ^2
0.38	0.49	0.22	0.29	0.01	56	1.15
0.25	0.43	0.29	0.28	0.01	56	1.12
0.25[b]	(0.43) ± 0.01	(0.28) ± 0.01	(0.28) ± 0.00	(0.01) ± 0.00	(56) ± 0	(0.96) ± 0.03
0.13	0.40	0.22	0.38	<0.01	56	1.20
0.07	0.31	0.33	0.36	<0.01	54	1.04

(c) Fractions of Pyrene Groups which Are either Present as Single Units (f_{diff} and f_{free}) or Involved into Lose Pyrene Aggregates (f_{agg}), Pyrene GS Dimers (f_{E1}) or Long-Lived Pyrene Dimers (f_{E2}) in THF

[Poly] (g/L)	f_{diff}	f_{free}[c]	f_{agg}	f_{E1}	f_{E2}[c]
0.38	0.23 ± 0.02	0.03	0.42 ± 0.05	0.31 ± 0.03	0.01
0.25	0.30 ± 0.02	0.05	0.36 ± 0.05	0.29 ± 0.02	0.01
0.13	0.22 ± 0.01	0.03	0.36 ± 0.03	0.39 ± 0.02	<0.01
0.07	0.29 ± 0.02	0.05	0.34 ± 0.04	0.32 ± 0.02	<0.01

[a] The parameters retrieved from the analysis of the monomer decay with a polymer concentration of 0.25 g/L with eq 4a were used to simulate 10 decays with different Poisson noise patterns, which were then fitted with eq 4a. The values in parentheses are the average. The error represents the standard deviation obtained for the 10 decays. [b] The parameters retrieved from the analysis of the excimer decay with a polymer concentration of 0.25 g/L with eq 4b were used to simulate 10 decays with different Poisson noise patterns, which were then fitted with eq 4b. The values in parentheses are the average. The error represents the standard deviation obtained for the 10 decays. [c] Error is smaller than ± 0.01.

pyrene monomer $[Py^*]_{(t)}$ and the pyrene excimer $[E^*]_{(t)}$ are given in eqs 4a and 4b

$$[Py^*]_{(t)} = [Py^*_{agg}]_{(t)} + [Py^*_{diff}]_{(t)} + [Py^*_{free}]_{(t)} = [Py^*_{agg}]_{(t=0)} e^{-(k_{agg} + 1/\tau_M)t} + [Py^*_{diff}]_{(t=0)} e^{-1/\tau_M} + [Py^*_{diff}]_{(t=0)} \times \exp\left[-\left(A_2 + \frac{1}{\tau_M}\right)t - A_3 (1 - \exp(-A_4 t))\right] \quad (4a)$$

$$[E^*]_{(t)} = [E1^*]_{(t)} + [E2^*]_{(t)} = -\frac{k_{agg}[Py^*_{agg}]_{(t=0)}}{k_{agg} + \frac{1}{\tau_M} - \frac{1}{\tau_{E1}}} \times e^{-(k_{agg} + 1/\tau_M)t} - [Py^*_{diff}]_{(t=0)} e^{-A_3} \times \sum_{i=0}^{\infty} \frac{A_2 + iA_4}{A_2 + iA_4 + \frac{1}{\tau_M} - \frac{1}{\tau_{E1}}} e^{-[A_2 + iA_4 + 1/\tau_M]t} \frac{A_3^i}{i!} + \left([E1^*]_{(t=0)} + \frac{k_{agg}[Py^*_{agg}]_{(t=0)}}{k_{agg} + \frac{1}{\tau_M} - \frac{1}{\tau_{E1}}} + [Py^*_{diff}]_{(t=0)} e^{-A_3} \times \sum_{i=0}^{\infty} \frac{A_2 + iA_4}{A_2 + iA_4 + \frac{1}{\tau_M} - \frac{1}{\tau_{E1}}} \frac{A_3^i}{i!} \right) e^{-t/\tau_{E1}} + [E2^*]_{(t=0)} e^{-t/\tau_{E2}} \quad (4b)$$

The expressions of the parameters A_2, A_3, and A_4 are given in eq 5,[11]

$$A_2 = \langle n \rangle \frac{k_{diff} k_e[blob]}{k_{diff} + k_e[blob]}$$

$$A_3 = \langle n \rangle \frac{k_{diff}^2}{(k_{diff} + k_e[blob])^2}$$

$$A_4 = k_{diff} + k_e[blob] \quad (5)$$

where k_{diff}, k_e[blob], and $\langle n \rangle$ represent the rate constant of excimer formation inside a *blob* containing one excited pyrene and one GS pyrene, the rate at which pyrene groups exchange from *blob* to *blob*, and the average number of quenchers Q per *blob*, respectively.

The fluorescence decays of the pyrene monomer were first analyzed with eq 4a. The fit yielded the rate constant for excimer formation inside a loose pyrene aggregate k_{agg}, the normalized preexponential weights f_{Mdiff}, f_{Magg},and f_{Mfree} and the parameters k_{diff}, k_e[blob], and $\langle n \rangle$ which are listed in Table 2a. The expressions of f_{Mdiff}, f_{Magg}, and f_{Mfree} are given in eqs 6a−c.

$$f_{Mdiff} = \frac{[Py^*_{diff}]_{(t=0)}}{[Py^*_{diff}]_{(t=0)} + [Py^*_{agg}]_{(t=0)} + [Py^*_{free}]_{(t=0)}} \quad (6a)$$

$$f_{Magg} = \frac{[Py^*_{agg}]_{(t=0)}}{[Py^*_{diff}]_{(t=0)} + [Py^*_{agg}]_{(t=0)} + [Py^*_{free}]_{(t=0)}} \quad (6b)$$

$$f_{Mfree} = \frac{[Py^*_{free}]_{(t=0)}}{[Py^*_{diff}]_{(t=0)} + [Py^*_{agg}]_{(t=0)} + [Py^*_{free}]_{(t=0)}} \quad (6c)$$

The fits were good and all χ^2 were smaller than 1.20. In the low concentration range studied (0.07 g/L < [EP−Py] < 0.38 g/L), the parameters retrieved from the analysis are constant

SCHEME 3: Photochemical Processes Taking Place in THF between the Pyrene Moieties[a]

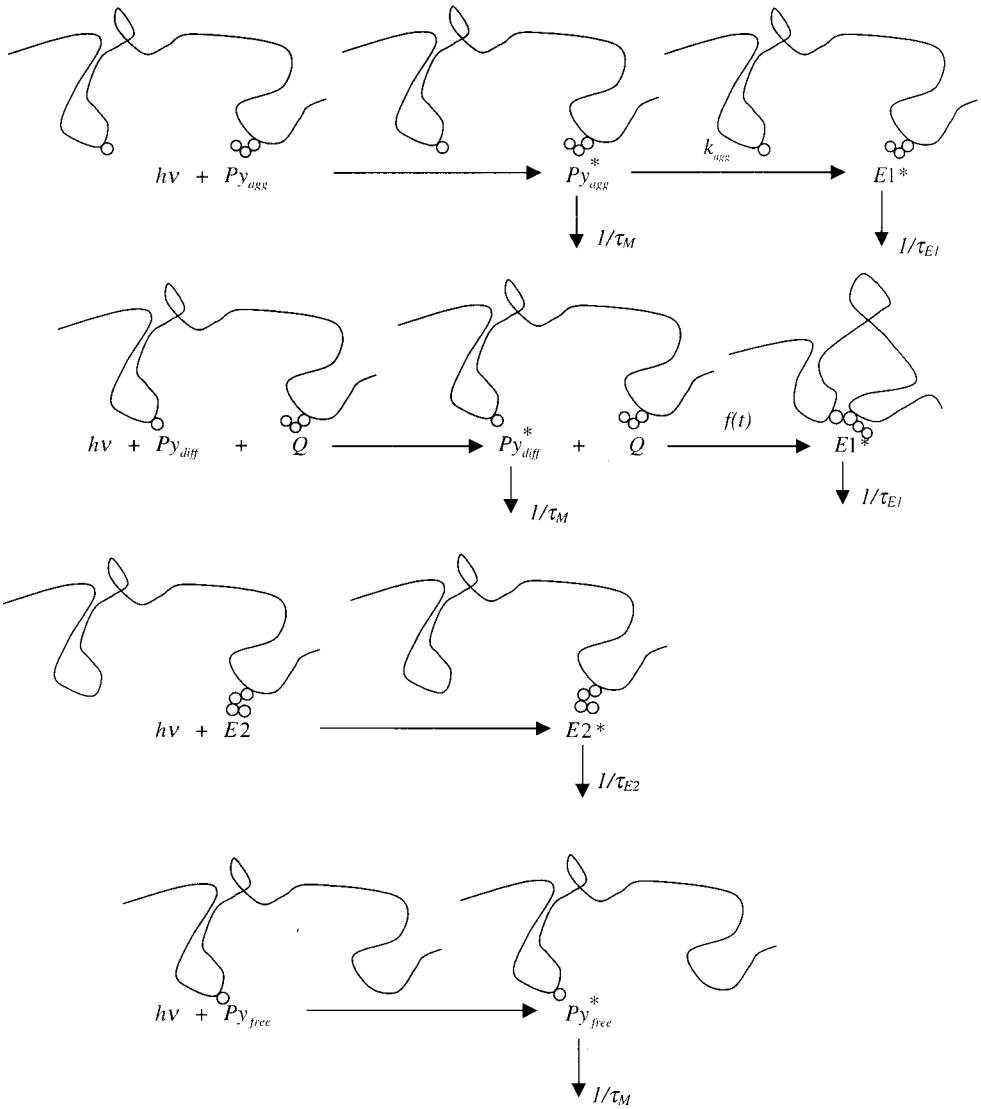

[a] The circles represent individual MA units.

within experimental error. They show that the rate of excimer formation inside a loose pyrene aggregate is large as expected from pyrene groups located inside a small volume. It equals $(14.2 \pm 1.9) \times 10^7$ s^{-1}, which is comparable to what was obtained in several other studies.[14,17] The parameters describing the diffusion controlled encounters equal $(1.6 \pm 0.3) \times 10^7$ s^{-1}, $(0.2 \pm 0.1) \times 10^7$ s^{-1}, and (1.8 ± 0.1) for k_{diff}, k_e[blob], and $\langle n \rangle$, respectively. These values are reasonable.[11,17] The contribution arising from unquenched pyrene is small and amounts to 0.06±0.01, indicating that most pyrene groups produce excimers. The ratio f_{Magg}/f_{Mdiff}, which represents the quantity $[Py^*_{agg}]_{(t=0)}/[Py^*_{diff}]_{(t=0)}$, equals 1.3 ± 0.3.

Since a pyrene GS dimer is excited instantaneously by the direct absorption of a photon, pyrene groups involved into pyrene GS dimers cannot be accounted for in the monomer decays. However, they can be detected in the excimer decays by monitoring the intensity of the excimer decay at time $t = 0$. If no counts are recorded at time $t = 0$, no ground-state dimer is present. The larger the number of counts recorded at time $t = 0$ and the more ground-state dimers are present. To obtain a complete overview of the pyrene population, the thorough analysis of the excimer decays is required. First, eq 4b was used to fit the excimer decays without assuming the presence of long-lived pyrene dimers, i.e., setting $[E2^*]_{(t=0)}$ to equal 0.0. The parameters k_{agg}, A_2, A_3, and A_4, which were obtained from the fit of the monomer fluorescence decays, were input into eq 4b and their values were fixed in the excimer decay analysis. In so doing the modified eq 4b becomes a linear sum of four functions. A General Linear Least Squares routine was used to fit the excimer decays.[19b] The fitting software optimized the excimer lifetime τ_{E1} using a Golden Section Search.[19c] Although the fits were good at the early times, some distortions were visible at longer times.

Equations 3a−d are based on the assumption that all the nonradiative energy lost by the pyrene monomer (i.e., all decay processes other than $1/\tau_M$) results in the formation of the excimer E1* with a lifetime τ_{E1}. Since poor fits of the excimer fluorescence decays are obtained at longer times using this assumption, we concluded that another physical process is taking place at longer times, which does not involve the pyrene monomer. This led us to assume the presence of long-lived excited pyrene dimers (E2*).

The presence of long-lived dimers is not unexpected in dye aggregates. An excimer is the result of the perfect stacking between an excited dye and a GS one.[5,12] In order for such a perfect stacking to occur, the dyes must have enough freedom to rearrange themselves. This is certainly not the case inside a dye aggregate where dyes pile up in a disordered fashion and

TABLE 3

(a) Parameters Retrieved from the Four-Exponential Fit of the Pyrene Monomer Fluorescence Decays of EP−Py in Hexane (λ_{ex} = 344 nm, λ_{em} = 377 nm)

[Poly] (g/L)	a_{M1}	τ_{M1} (ns)	a_{M2}	τ_{M2} (ns)	a_{M3}	τ_{M3} (ns)	a_{M4}	τ_{M4} (ns)	χ^2
0.15	0.57	3.5	0.25	18	0.08	94	0.11	260	1.13
0.04	0.60	3.1	0.22	17	0.08	86	0.11	260	1.08
0.03	0.59	4.4	0.22	21	0.08	102	0.11	260	1.10
0.01	0.50	5.3	0.20	24	0.09	95	0.22	260	0.95

(b) Parameters Retrieved from the Tri-Exponential Fit of the Pyrene Excimer Fluorescence Decays of EP−Py in Hexane (λ_{ex} = 344 nm, λ_{em} = 520 nm)

[Poly] (g/L)	a_{E1}	τ_{E1} (ns)	a_{E2}	τ_{E2} (ns)	a_{E3}	τ_{E3} (ns)	χ^2
0.15	−0.18	7.5	1.00	63	0.01	184	1.10
0.04	−0.17	7.1	1.00	62	0.02	159	1.30
0.03	−0.24	9.3	1.00	59	0.13	95	1.00
0.01	−0.27	8.5	1.00	63	0.03	148	1.10

where their motions are constrained by the polymer backbone. Such dye aggregates can generate low-energy dimers, which fluoresce with a longer lifetime. For instance, naphthalene long-lived dimers have been detected in a poly(ethylene terephthalate-*co*-2,6-naphthalene dicarboxylate) matrix where the high concentration of naphthalene dyes leads to the formation of naphthalene aggregates.[21] A recent report describes long-lived pyrene dimers, which are generated during the coil-to-globule collapse of a polymer coil.[22]

The triexponential fits of the pyrene excimer fluorescence decays in THF (cf. Table 1b) and in hexane (cf. Table 3b) do indicate the presence of a long-lived component ($\tau_{E3} > 100$ ns). Because its contribution to the excimer decays is small, it cannot be determined accurately. Consequently, the lifetime of the long-lived pyrene dimers (τ_{E2}) was arbitrarily fixed to equal 150 ns in the analysis of the excimer fluorescence decays with the complete eq 4b. Again, a General Linear Least Squares routine was used to fit the excimer decays and the optimization of the χ^2 parameter was performed by applying a Golden Section Search to the excimer lifetime τ_{E1}.[19b,c] The fits were good ($\chi^2 < 1.20$) and yielded the excimer lifetime τ_{E1} and the fractions f_{Eagg}, f_{Ediff}, f_{EE1}, and f_{EE2} whose expressions are given in eqs 7a−d.

$$f_{Ediff} = \frac{[Py^*_{diff}]_{(t=0)}}{[Py^*_{diff}]_{(t=0)} + [Py^*_{agg}]_{(t=0)} + [E1^*]_{(t=0)} + [E2^*]_{(t=0)}} \quad (7a)$$

$$f_{Eagg} = \frac{[Py^*_{agg}]_{(t=0)}}{[Py^*_{diff}]_{(t=0)} + [Py^*_{agg}]_{(t=0)} + [E1^*]_{(t=0)} + [E2^*]_{(t=0)}} \quad (7b)$$

$$f_{EE1} = \frac{[E1^*]_{(t=0)}}{[Py^*_{diff}]_{(t=0)} + [Py^*_{agg}]_{(t=0)} + [E1^*]_{(t=0)} + [E2^*]_{(t=0)}} \quad (7c)$$

$$f_{EE2} = \frac{[E2^*]_{(t=0)}}{[Py^*_{diff}]_{(t=0)} + [Py^*_{agg}]_{(t=0)} + [E1^*]_{(t=0)} + [E2^*]_{(t=0)}} \quad (7d)$$

The values of the parameters τ_{E1}, f_{Eagg}, f_{Ediff}, f_{EE1}, and f_{EE2} retrieved from the analysis of the excimer decays with the complete eq 4b are listed in Table 2b. The excimer lifetime was found to equal 55 ± 1 ns, which is reasonable for the pyrene excimer.[5] The contribution from the long-lived pyrene dimers was indeed very small, never larger than 0.01. The ratio f_{Eagg}/f_{Ediff} which represents the quantity $[Py^*_{agg}]_{(t=0)}/[Py^*_{diff}]_{(t=0)}$, equals 1.6 ± 0.6. Within experimental error, it equals the ratio f_{Magg}/f_{Mdiff} obtained from the monomer decay analysis with eq 4a.

Equations 6a−c and 7a−d can now be rearranged into eqs 8a−e to yield the complete distribution of pyrene groups among the different species Py^*_{diff}, Py^*_{agg}, Py^*_{free}, E1*, and E2*.

$$f_{diff} = \frac{[Py^*_{diff}]_{(t=0)}}{[Py^*_{diff}]_{(t=0)} + [Py^*_{free}]_{(t=0)} + [Py^*_{agg}]_{(t=0)} + [E1^*]_{(t=0)} + [E2^*]_{(t=0)}} \quad (8a)$$

$$f_{free} = \frac{[Py^*_{free}]_{(t=0)}}{[Py^*_{diff}]_{(t=0)} + [Py^*_{free}]_{(t=0)} + [Py^*_{agg}]_{(t=0)} + [E1^*]_{(t=0)} + [E2^*]_{(t=0)}} \quad (8b)$$

$$f_{agg} = \frac{[Py^*_{agg}]_{(t=0)}}{[Py^*_{diff}]_{(t=0)} + [Py^*_{free}]_{(t=0)} + [Py^*_{agg}]_{(t=0)} + [E1^*]_{(t=0)} + [E2^*]_{(t=0)}} \quad (8c)$$

$$f_{E1} = \frac{[E1^*]_{(t=0)}}{[Py^*_{diff}]_{(t=0)} + [Py^*_{free}]_{(t=0)} + [Py^*_{agg}]_{(t=0)} + [E1^*]_{(t=0)} + [E2^*]_{(t=0)}} \quad (8d)$$

$$f_{E2} = \frac{[E2^*]_{(t=0)}}{[Py^*_{diff}]_{(t=0)} + [Py^*_{free}]_{(t=0)} + [Py^*_{agg}]_{(t=0)} + [E1^*]_{(t=0)} + [E2^*]_{(t=0)}} \quad (8e)$$

The results are listed in Table 2c. Within experimental error, it is found that the fractions f_{diff}, f_{free}, f_{agg}, f_{E1}, and f_{E2} equal 0.26 ± 0.04, 0.04 ± 0.01, 0.37 ± 0.06, 0.33 ± 0.05, and <0.01, respectively. According to these results, there are three main contributions to the fluorescence decays. The first major contribution arises from the pyrene groups, which are attached as single units (f_{diff} = 0.26 ± 0.04). The second major contribution arises from pyrene groups, which are involved into loose pyrene aggregates but behave as pyrene monomers and form excimer with the rate constant k_{agg} (f_{agg} = 0.37 ± 0.06). The third major contribution arises from pyrene groups which are involved into pyrene GS dimers, which form excimer E1* instantaneously upon excitation (f_{E1} = 0.33 ± 0.05). Consequently 67% of the excitation photons ($f_{diff} + f_{free} + f_{agg}$) will excite pyrene monomers and 33% of the excitation photons ($f_{E1} + f_{E2}$) will excite pyrene GS dimers. Since two-thirds of the pyrene groups behave as pyrene monomers, a good overlap of the excitation spectra of the monomer and the excimer is expected, as was observed by Vangani et al.[17] The fraction of pendants, which are attached as single units onto the polymer backbone, equals $f_{diff} + f_{free}$ = 0.30. This indicates that most pendants in this maleated EP copolymer (70% of them) are

SCHEME 4: Representation of EP−Py in Hexane[a]

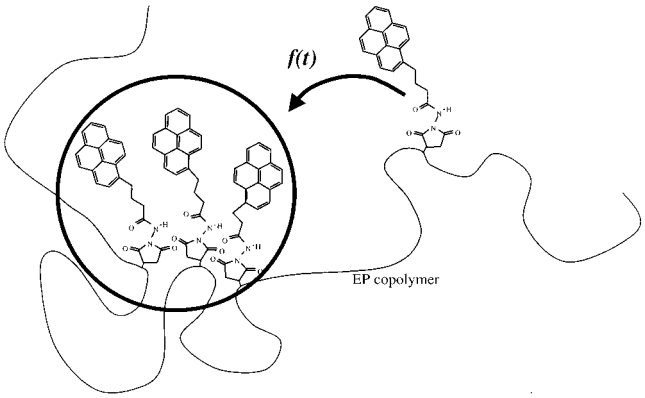

[a] Polar associations between the polar MA units induce the formation of loose pyrene aggregates shown as a solid circle. The function $f(t)$ describes the rate of encounter between pyrene groups randomly distributed along the polymer backbone.

attached either as oligoMA or on different but neighboring polymer units.

Equations 4a and 4b might look complicated, since they depend on seven parameters for the monomer and the same seven parameters plus three new parameters for the excimer. This large number of independent parameters might rise some legitimate concern about overinterpreting the fluorescence data. To address this concern, some monomer fluorescence decays were simulated with added Poisson noise.[20] Their analysis with eq 4a showed that the analysis software was able to retrieve the input parameters with a reasonable accuracy, as shown in Table 2a for an EP−Py concentration of 0.25 g/L. Excimer fluorescence decays were simulated as well. Our analysis of the simulated excimer decay with eq 4b recovered the input parameters with satisfying accuracy as can be seen in Table 2b for an EP−Py concentration of 0.25 g/L.

At this stage of the report, the microstructure of the maleated EP copolymer has been established. In the following section, the association level of the copolymer is investigated by monitoring how the distribution of species evolves when the solvent is changed from polar THF to apolar hexane.

Associative Strength of the Maleated EP Copolymer. In an earlier report, a concentration study of EP−Py has been carried out in hexane.[17] The monomer and excimer decays were recorded, but only the monomer decays were studied in a quantitative manner. In this work, both the monomer and excimer decays are studied in a quantitative manner in order to obtain a complete description of the system. The fluorescence decay measurements carried out at low polymer concentration (0.01 g/L < [EP−Py] < 0.15 g/L) in hexane are being considered for comparison with the decays in THF, which were obtained at similar polymer concentrations. In this polymer concentration range, excimer formation is expected to occur mostly intramolecularly. Figure 2 shows the typical fluorescence decays of EP−Py monomer and excimer in hexane.

In apolar hexane, the polar succinic anhydride pendants are expected to promote polar associations, which generate loose pyrene aggregates (cf. Scheme 4). This was indeed observed by Vangani et al. and the following paragraph is a brief summary of their findings.[17] The monomer and excimer decays were fitted with four and three exponentials, respectively. The decaytimes and preexponential factors retrieved from the analysis are listed in Table 3. The excimer decays exhibit a fast rise time τ_{E1}, which equals 8.1 ± 1.0 ns. It is paralleled by a short decaytime τ_{M1} in the monomer decays. This indicates that excimers are being formed on a fast time scale, which is expected if loose pyrene aggregates are present. In the excimer decays, the ratio $a_{E1}/(a_{E2} + a_{E3})$ equals −0.20 ± 0.03. This indicates that more pyrene GS dimers are present in hexane than in THF where the same ratio equals −0.54 ± 0.05. This is again expected since apolar hexane promotes associations between the grafted MA units. The second decaytime of the excimer τ_{E2} equals 60 ± 1 ns, which is a typical value for the excimer lifetime.[5] In the monomer decays, the fourth decaytime τ_{M4} is fixed to equal 260 ns, which is the lifetime (τ_M) of a single PHZ attached onto a maleated polyolefin in hexane.[14] The contribution of the fourth exponential is due to unquenched pyrene monomer. It is small and equals 0.14 ± 0.06. As was observed for the excimer decays in THF, all excimer decays in hexane require a long decaytime ($\tau_{E3} > 95$ ns) to yield good fits. The long decaytime τ_{E3} could be due to the presence of a small population of long-lived pyrene dimers. The decaytimes τ_{M2} and τ_{M3} in the monomer decays represent slower relaxation processes, which do not occur inside a loose pyrene aggregate. This slower relaxation processes are certainly due to diffusion controlled encounters between a single excited pyrene and another pyrene species (GS pyrene monomer or a loose pyrene aggregate) located on the backbone.

To take into account all the factors listed above, Scheme 5 is introduced. Scheme 5 was already used to fit the fluorescence decays of the pyrene monomer in hexane, but it has never been applied to the excimer decays.[17] Scheme 5 assumes that excimer formation occurs in a sequential manner. First diffusional encounters between a single excited pyrene group (Py^*_{diff}) and either a single GS pyrene (Py_{diff}) or a GS pyrene aggregate (Py_{agg}) attached on the polymer backbone lead to the formation of an excited pyrene aggregate (Py^*_{agg}). Py^*_{agg} can be formed via either polar interactions between the MA pendants as shown in Scheme 4 or from the PHZ labeling of oligoMA, as shown in Scheme 1. However, our analysis is unable to distinguish between loose pyrene aggregates due to polar associations or oligoMA. Consequently both types are referred to as Py^*_{agg}. Inside a loose pyrene aggregate, the pyrene groups rearrange quickly with a rate constant k_{agg} to yield an excimer E1*. Because many pyrene groups are concentrated inside a loose pyrene aggregate, pyrene GS dimers (E1) and long-lived pyrene dimers (E2) are expected to be present as well. Due to the random MA grafting along the polyolefin, the distribution of distances between grafted species generates a distribution of encounter rate constants. As a result the rate for diffusional encounters is given by the function $f(t)$. The time dependent behaviors of Py^*_{diff}, Py^*_{agg}, Py^*_{free}, E1*, and E2* are described in the five following differential equations:

$$\frac{d[Py^*_{agg}]}{dt} = f(t) - \left(k_{agg} + \frac{1}{\tau_M}\right)[Py^*_{agg}] \quad (9a)$$

$$\frac{d[Py^*_{agg}]}{dt} = -\frac{1}{\tau_M}[Py^*_{free}] \quad (9b)$$

$$\frac{d[Py^*_{diff}]}{dt} = -f(t) - \frac{1}{\tau_M}[Py^*_{diff}] \quad (9c)$$

$$\frac{d[E1^*]}{dt} = k_{agg}[Py^*_{agg}] - \frac{1}{\tau_{E1}}[E1^*] \quad (9d)$$

$$\frac{d[E2^*]}{dt} = -\frac{1}{\tau_{E2}}[E2^*] \quad (9e)$$

The differential eqs 9a−e were solved in a manner very similar to the one used earlier on for eqs 3a−e and their integration is described in more detail in Appendix B. The function $f(t)$, which represents the rate at which pyrene groups randomly located along the backbone encounter one another, was estimated by using the *blob* model.[11,17] Integration of eqs 9a−e yields the time-dependent behavior of the pyrene monomer and excimer given in eqs 10a and 10b.

$$[\mathrm{Py}^*]_{(t)} = [\mathrm{Py}^*_{\mathrm{agg}}]_{(t)} + [\mathrm{Py}^*_{\mathrm{diff}}]_{(t)} + [\mathrm{Py}^*_{\mathrm{free}}]_{(t)} =$$

$$\left([\mathrm{Py}^*_{\mathrm{agg}}]_{(t=0)} + [\mathrm{Py}^*_{\mathrm{diff}}]_{(t=0)}\mathrm{e}^{-A_3}\sum_{i=0}^{\infty}\frac{A_3^i}{i!}\frac{A_2 + iA_4}{A_2 + iA_4 - k_{\mathrm{agg}}}\right) \times$$

$$\mathrm{e}^{-(k_{\mathrm{agg}} + 1/\tau_{\mathrm{M}})t} - [\mathrm{Py}^*_{\mathrm{diff}}]_{(t=0)}\mathrm{e}^{-A_3} \times$$

$$\sum_{i=0}^{\infty}\frac{A_3^i}{i!}\frac{k_{\mathrm{agg}}}{A_2 + iA_4 - k_{\mathrm{agg}}}\mathrm{e}^{-(A_2 + iA_4 + 1/\tau_M)t} + [\mathrm{Py}^*_{\mathrm{free}}]_{(t=0)}\mathrm{e}^{-1/\tau_M} \quad (10a)$$

$$[\mathrm{E}^*]_{(t)} = [\mathrm{E1}^*]_{(t)} + [\mathrm{E2}^*]_{(t)} =$$

$$-\left([\mathrm{Py}^*_{\mathrm{agg}}]_{(t=0)} + [\mathrm{Py}^*_{\mathrm{diff}}]_{(t=0)}\mathrm{e}^{-A_3}\sum_{i=0}^{\infty}\frac{A_3^i}{i!}\frac{A_2 + iA_4}{A_2 + iA_4 - k_{\mathrm{agg}}}\right) \times$$

$$\frac{k_{\mathrm{agg}}}{k_{\mathrm{agg}} + \dfrac{1}{\tau_{\mathrm{M}}} - \dfrac{1}{\tau_{\mathrm{E1}}}}\mathrm{e}^{-(k_{\mathrm{agg}} + 1/\tau_{\mathrm{M}})t} +$$

$$[\mathrm{Py}^*_{\mathrm{diff}}]_{(t=0)}\mathrm{e}^{-A_3}\sum_{i=0}^{\infty}\frac{A_3^i}{i!}\frac{A_2 + iA_4}{A_2 + iA_4 - k_{\mathrm{agg}}} \times$$

$$\frac{k_{\mathrm{agg}}}{A_2 + iA_4 + \dfrac{1}{\tau_{\mathrm{M}}} - \dfrac{1}{\tau_{\mathrm{E1}}}}\mathrm{e}^{-(A_2 + iA_4 + 1/\tau_{\mathrm{M}})t} +$$

$$\left[[\mathrm{E1}^*]_{(t=0)} - [\mathrm{Py}^*_{\mathrm{diff}}]_{(t=0)}\mathrm{e}^{-A_3}\sum_{i=0}^{\infty}\frac{A_3^i}{i!}\frac{A_2 + iA_4}{A_2 + iA_4 - k_{\mathrm{agg}}} \times \right.$$

$$\frac{k_{\mathrm{agg}}}{A_2 + iA_4 + \dfrac{1}{\tau_{\mathrm{M}}} - \dfrac{1}{\tau_{\mathrm{E1}}}} + \frac{k_{\mathrm{agg}}}{k_{\mathrm{agg}} + \dfrac{1}{\tau_{\mathrm{M}}} - \dfrac{1}{\tau_{\mathrm{E1}}}} \times$$

$$\left.\left([\mathrm{Py}^*_{\mathrm{agg}}]_{(t=0)} + [\mathrm{Py}^*_{\mathrm{diff}}]_{(t=0)}\mathrm{e}^{-A_3}\sum_{i=0}^{\infty}\frac{A_3^i}{i!}\frac{A_2 + iA_4}{A_2 + iA_4 - k_{\mathrm{agg}}}\right) \times \right]$$

$$\mathrm{e}^{-t/\tau_{\mathrm{E1}}} + [\mathrm{E2}^*]_{(t=0)}\mathrm{e}^{-t/\tau_{\mathrm{E2}}} \quad (10b)$$

The expressions of the parameters A_2, A_3, and A_4 have been given in eq 5. As for eqs 4a and 4b, eqs 10a and 10b might look complicated but they really depend on only a few parameters, seven for 10a and the same seven plus three new parameters for 10b. The fluorescence decays were fitted according to the same procedure used for eqs 4a and 4b). First, the fluorescence decays of the pyrene monomer were fitted with eq 10a to yield k_{agg}, the normalized preexponential weights f_{Mdiff}, f_{Magg}, and f_{Mfree} and k_{diff}, k_{e}[blob], and $\langle n\rangle$ which are listed in Table 4a. The expressions of f_{Mdiff}, f_{Magg}, and f_{Mfree} were given in eqs 6a−c. The parameters retrieved from the analysis of the fluorescence decays with eq 10a are constant with concentration within experimental error. f_{Mdiff}, f_{Magg}, f_{Mfree} k_{agg}, k_{diff}, k_{e}[blob], and $\langle n\rangle$ equal 0.30 ± 0.03, 0.56 ± 0.02, 0.14 ± 0.03, (19.5 ± 2.3) × 10^7 s^{-1}, (2.1 ± 0.4) × 10^7 s^{-1}, (0.4 ± 0.04) × 10^7 s^{-1}, and 1.7 ± 0.2, respectively. The rate of excimer formation inside a loose pyrene aggregate is large [(19.5 ± 2.3) × 10^7 s^{-1}] and takes a value comparable to but slightly larger than the one obtained in THF [(14.2 ± 1.9) × 10^7 s^{-1}]. The same is observed for k_{diff}, which equals (2.1 ± 0.4) × 10^7 s^{-1} in hexane and (1.6 ± 0.3) × 10^7 s^{-1} in THF. This trend can be explained by taking into account solvent viscosity. The viscosity of hexane at 25 °C is 0.30 mPa.s. THF is 50% more viscous with a viscosity of 0.45 mPa·s at 25 °C and lower rate constants are being retrieved in THF. The parameters describing the diffusion controlled process, namely k_{diff}, k_{e}[blob], and $\langle n\rangle$, yield values, which are close to those obtained for EP−Py in THF and are similar to those obtained with polystyrene samples.[11] The ratio $f_{\mathrm{Magg}}/f_{\mathrm{Mdiff}}$ equals 1.9 ± 0.2 which indicates that the concentration of pyrene monomers emitting from a loose pyrene aggregate is about twice that of pyrene monomer attached onto isolated succinic anhydride units.

To obtain a complete overview of all species present in solution, the excimer decays must be analyzed to account for the contribution of the GS dimers. To this effect, the parameters k_{agg}, k_{diff}, k_{e}[blob], and $\langle n\rangle$ obtained from the analysis of the monomer fluorescence decays were fixed in eq 10b. Equation 10b becomes then a linear sum of four functions, where the only unknowns are $[\mathrm{Py}^*_{\mathrm{diff}}]_{(t=0)}$, $[\mathrm{Py}^*_{\mathrm{agg}}]_{(t=0)}$, $[\mathrm{E1}^*]_{(t=0)}$, $[\mathrm{E2}^*]_{(t=0)}$, τ_{E1}, and τ_{E2}. A first analysis of the excimer fluorescence decays carried out with the assumption that no long-lived pyrene dimers were present (i.e., $[\mathrm{E2}^*]_{(t=0)} = 0.0$) yielded poor fits at the longer times. Consequently a contribution from long-lived pyrene dimers was introduced for the analysis of the excimer decays. As for the excimer fluorescence decays in THF, the lifetime of the long-lived pyrene dimers could not be determined with sufficient accuracy. It was fixed arbitrarily in the analysis to equal 150 ns. The analysis yielded the parameters τ_{E1}, f_{Eagg}, f_{Ediff}, f_{EE1}, and f_{EE2}, which are listed in Table 4b and whose expressions were given in eqs 7a−d.

The excimer lifetime τ_{E1} was found to equal 61 ± 1 ns, which is reasonable for the lifetime of the pyrene excimer.[5] It is also in very good agreement with the excimer lifetime obtained for a maleated oligo(isobutylene) labeled at a single end with PHZ in hexane.[14] Whereas the monomer fluorescence decays obtained in hexane are very comparable to those obtained in THF, the excimer decays obtained in hexane show a very different behavior from the ones observed in THF. In hexane, f_{EE1} equals 0.72 ± 0.06, whereas it equals 0.34 ± 0.06 in THF. This clearly indicates that there are many more pyrene GS dimers in hexane than in THF. Unfortunately the importance of the GS dimer contribution in hexane dwarfs the contributions of the other species, i.e., $\mathrm{Py}^*_{\mathrm{diff}}$, $\mathrm{Py}^*_{\mathrm{agg}}$, $\mathrm{Py}^*_{\mathrm{free}}$, and E2*, which are obtained with less accuracy. In particular, f_{Ediff}, which should equal about half f_{Eagg} according to the analysis of the monomer decays (cf.

SCHEME 5: Photochemical Processes Taking Place in Hexane between the Pyrene Moieties of EP−Py[a]

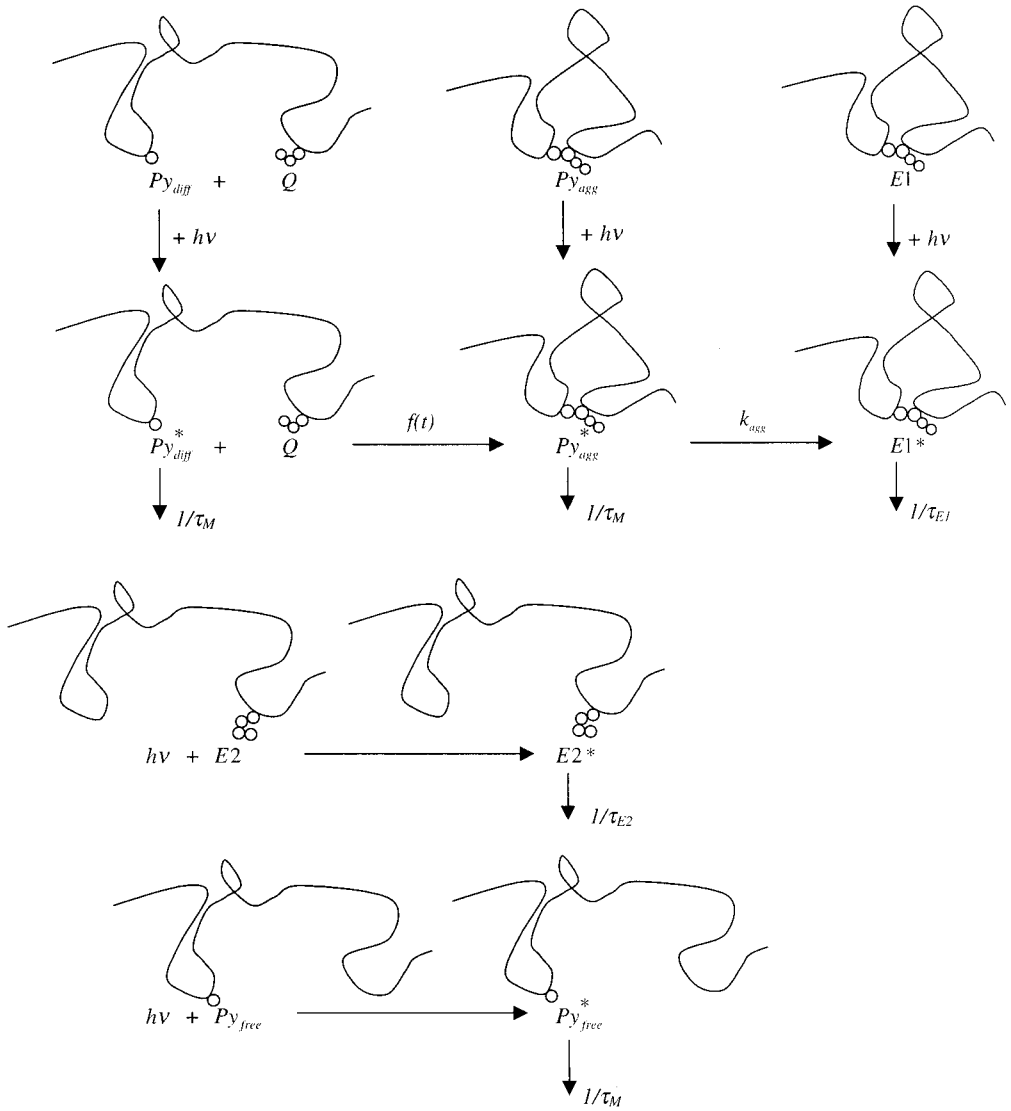

[a] The circles represent individual MA units.

Table 4a), is obtained with little accuracy ($f_{Ediff} = 0.06 \pm 0.04$ in Table 4b). As a result, f_{Ediff} was not used in order to determine the fractions f_{diff}, f_{free}, f_{agg}, f_{E1}, and f_{E2}, which are listed in Table 4c and whose expressions were given in eqs 8a−e.

Within experimental error, the values of f_{diff}, f_{free}, f_{agg}, f_{E1}, and f_{E2} remain constant over the polymer concentration range and equal 0.09 ± 0.02, 0.04 ± 0.02, 0.17 ± 0.04, 0.67 ± 0.07, 0.02 ± 0.01, respectively. According to this analysis, the fraction of pyrene groups involved into pyrene GS dimers doubles when the solvent is switched from polar THF ($f_{E1} + f_{E2} = 0.33$) to apolar hexane ($f_{E1} + f_{E2} = 0.69$). This certainly explains why the excitation spectra of the pyrene monomer and excimer exhibit such a large shift in hexane and not in THF.[17] In hexane only 13% of all pyrene groups ($f_{diff} + f_{free}$) remain as single units attached along the polymer backbone. This fraction is half that obtained in THF where ($f_{diff} + f_{free}$) equals 0.30. In hexane most pyrene groups are involved into loose pyrene aggregates and the fraction of associated pendants $f_{AP} = f_{agg} + f_{E1} + f_{E2}$ equals 0.87.

This apparently large number however does not demonstrate that hexane promotes associations between polar pendants of EP−Py because the microstructure of the polymer obtained in THF indicates that already 70% of all pendants are either involved into oligoMA or attached to nearby polymer units. The associative strength of this type of polar pendant was well established with an oligo(isobutylene) labeled at one end with PHZ.[14] In that work, switching from polar THF to apolar hexane increased f_{AP} from 0.20 to >0.95.

Finally the accuracy of eqs 10a and 10b was investigated by analyzing monomer and excimer fluorescence decays, which were simulated with added Poisson noise. The results given in Tables 4a and 4b for the monomer and the excimer, respectively, show that our software retrieve the parameters of interest with reasonable accuracy.

Conclusion

In this paper, the importance of characterizing the microstructure of an AP before studying its associative strength was emphasized. Two mathematical treatments were proposed to achieve these two objectives by fluorescence spectroscopy. They are based on the combination of a *sequential* and a *blob* model. Using these tools, the microstructure and the associative strength (defined as the fraction of associated pendants versus the fraction of unassociated pendants) of a maleated EP copolymer were

TABLE 4

(a) Parameters Retrieved from Fitting the Pyrene Monomer Fluorescence Decays of EP−Py in Hexane with eq 4a

[Poly] (g/L)	f_{Magg}	f_{Mdiff}	f_{Mfree}	k_{agg} (10^7 s^{-1})	$\langle n \rangle$	k_{diff} (10^7 s^{-1})	k_e[blob] (10^7 s^{-1})	χ^2
0.15	0.55	0.34	0.12	22.9	1.7	2.6	0.3	1.13
0.15[a]	(0.55) ± 0.02	(0.34) ± 0.03	(0.12) ± 0.01	(23.4) ±3.5	(1.7) ± 0.1	(2.6) ± 0.3	(0.3) ± 0.0	(0.95) ± 0.03
0.04	0.56	0.30	0.14	18.1	1.7	2.0	0.4	1.06
0.03	0.58	0.28	0.13	18.8	1.8	2.2	0.4	1.08
0.01	0.54	0.28	0.18	18.1	1.4	1.6	0.4	0.95

(b) Parameters Retrieved from Fitting the Pyrene Excimer Fluorescence Decays of EP−Py in Hexane with eq 5b

[Poly] (g/L)	f_{Eagg}	f_{Ediff}	f_{EE1}	f_{EE2}	τ_{E1} (ns)	χ^2
0.15	0.15	0.08	0.74	0.02	61	1.18
0.15[b]	(0.16) ± 0.02	(0.08) ± 0.01	(0.75) ± 0.01	(0.02) ± 0.00	(61) ± 0	(0.96) ± 0.03
0.04	0.15	0.03	0.79	0.03	61	1.28
0.03	0.25	0.01	0.72	0.01	62	1.14
0.01	0.24	0.11	0.64	0.02	60	1.20

(c) Fractions of Pyrene Groups which Are either Present as Single Units (f_{diff} and f_{free}) or Involved into Loose Pyrene Aggregates (f_{agg}), Pyrene GS Dimers (f_{E1}) or Long-Lived Pyrene Dimers (f_{E2}) in Hexane

[Poly] (g/L)	f_{diff}	f_{free}	f_{agg}	f_{E1}	f_{E2}
0.38	0.09	0.03	0.15	0.71	0.02
0.25	0.08	0.04	0.14	0.72	0.02
0.13	0.10	0.05	0.22	0.62	0.01
0.07	0.11	0.07	0.22	0.58	0.02

[a] The parameters retrieved from the analysis of the monomer decay with a polymer concentration of 0.15 g/L with eq 10a were used to simulate 10 decays with different Poisson noise patterns, which were then fitted with eq 10a. The values in parentheses are the average. The error represents the standard deviation obtained for the 10 decays. [b] The parameters retrieved from the analysis of the excimer decay with a polymer concentration of 0.15 g/L with eq 10b were used to simulate 10 decays with different Poisson noise patterns, which were then fitted with eq 10b. The values in parentheses are the average. The error represents the standard deviation obtained for the 10 decays.

determined. This analysis achieved a complete assignment of all the pyrene groups, which allows a detailled description of the AP system. In THF only 33% of the pyrene groups exist as preassociated GS dimers. In hexane this number rises to 69%. This explains why the excitation spectra of the monomer and of the excimer show a slight shift in THF (little preassociation) and a much larger shift in hexane (stronger preassociation).[17] It is for the same reason that the ratio of the excimer preexponential factors $a_{E1}/(a_{E2} + a_{E3})$ is more negative in THF where it equals -0.54 ± 0.05 than in hexane where it equals -0.20 ± 0.03. It was found that most MA units along the polyolefin are either present as oligoMA or attached to nearby polymeric units. Only 30% of the pendants were attached and behaved as single units. Switching the solvent from polar THF to apolar hexane reduces the fraction of unassociated pendants from 30% down to 13%, indicating enhanced association.

Our models assumed that long-lived excited dimers E2* are present and fluoresce with a long lifetime τ_{E2}. It is possible that E2* transforms into classic excimer E1* over time. However, the very small amount of E2* detected in our time-resolved fluorescence measurements ($f_{E2} < 2\%$) does not allow us to draw any conclusion on this issue. Since our models fitted the fluorescence decays satisfyingly without making this additional assumption, it was not implemented in our fitting procedure.

In the future, our ability to characterize the microstructure and association level of pyrene labeled APs will allow us to deepen our understanding on how these parameters are correlated with AP's viscoelastic properties. Although this work deals with the associative strength of a maleated EP copolymer, the same thought process can be applied to any other AP, where the associating pendants have been labeled with pyrene, as already done in numerous reports.[23]

Appendix A

The integration of eqs 3a−e is presented in more detail. Integration of eqs 3a, 3b, and 3e is trivial and yields

$$[Py^*_{agg}]_{(t)} = [Py^*_{agg}]_{(t=0)} e^{-(k_{agg} + 1/\tau_M)t} \quad \text{(A1)}$$

$$[Py^*_{free}]_{(t)} = [Py^*_{free}]_{(t=0)} e^{-t/\tau_M} \quad \text{(A2)}$$

$$[E2^*]_{(t)} = [E2^*]_{(t=0)} e^{-t/\tau_{E2}} \quad \text{(A3)}$$

The *blob* model is applied to account for the random distribution of quenchers along the polymer backbone. The polymer chain is divided into *blobs* among which pyrene groups distribute themselves randomly according to a Poisson distribution. According to Mathew et al.,[11] $[Py^*_{diff}]$ is given by eq A4,

$$[Py^*_{diff}]_{(t)} = [Py^*_{diff}]_{(t=0)} \times \exp\left[-\left(A_2 + \frac{1}{\tau_M}\right)t - A_3(1 - \exp(-A_4 t))\right]$$

$$= [Py^*_{diff}]_{(t=0)} e^{-A_3} \sum_{i=0}^{\infty} \frac{A_i^3}{i!} e^{-(A_2 + iA_4 + 1/\tau_M)t} \quad \text{(A4)}$$

where the expressions of A_2, A_3, and A_4 are given in eq 5. The two forms of eq A4 are equivalent and they are obtained by expanding the exponential into an infinite series. The complete expression for the excited pyrene monomer is obtained by summing up eqs A1, A2, and A4) to yield eq 4a in the main text.

To obtain the time-dependent behavior of $[E^*]_{(t)}$, an expression for the function $f(t)$ must be found. This is accomplished by expanding eq A4 into a sum of exponentials to yield eq A5.[17]

$$f(t) = -\frac{\mathrm{d}[\mathrm{Py}^*_{\mathrm{diff}}]}{\mathrm{d}t} - \frac{1}{\tau_{\mathrm{M}}}[\mathrm{Py}^*_{\mathrm{diff}}]_{(t)}$$

$$= [\mathrm{Py}^*_{\mathrm{diff}}]_{(t=0)} \mathrm{e}^{-A_3} \sum_{i=0}^{\infty} (A_2 + iA_4) \mathrm{e}^{-[A_2 + iA_4 + 1/\tau_{\mathrm{M}}]t} \frac{A_3^i}{i!} \quad \text{(A5)}$$

The expression of $f(t)$ can now be reinserted into eq 3d to yield, after integration, the time-dependent behavior of the excimer $[\mathrm{E1}^*]_{(t)}$. By adding the expression of $[\mathrm{E2}^*]_{(t)}$ given in eq (A3) to that of $[\mathrm{E1}^*]_{(t)}$, one obtains $[\mathrm{E}^*]_{(t)}$ given in eq 4b.

Appendix B

Integration of eqs 9b and 9e is trivial and yields

$$[\mathrm{Py}^*_{\mathrm{free}}]_{(t)} = [\mathrm{Py}^*_{\mathrm{free}}]_{(t=0)} \mathrm{e}^{-t/\tau_{\mathrm{M}}} \quad \text{(B1)}$$

$$[\mathrm{E2}^*]_{(t)} = [\mathrm{E2}^*]_{(t=0)} \mathrm{e}^{-t/\tau_{E2}} \quad \text{(B2)}$$

$[\mathrm{Py}^*_{\mathrm{diff}}]_{(t)}$ is obtained according to Mathew et al. and is given by eq A4.[11] It is then used to obtain the function $f(t)$ given by eq A5. In turn, the expression of the function $f(t)$ is then introduced into eq 9a to yield $[\mathrm{Py}^*_{\mathrm{agg}}]_{(t)}$.[17] Summing up eqs B1 for $[\mathrm{Py}^*_{\mathrm{free}}]_{(t)}$, B3 for $[\mathrm{Py}^*_{\mathrm{agg}}]_{(t)}$, and A4 for $[\mathrm{Py}^*_{\mathrm{diff}}]_{(t)}$ yields $[\mathrm{Py}^*]_{(t)}$ given in eq 10a.

$$[\mathrm{Py}^*_{\mathrm{diff}}]_{(t)} = -[\mathrm{Py}^*_{\mathrm{diff}}]_{(t=0)} \mathrm{e}^{-A_3} \times \sum_{i=0}^{\infty} \frac{A_3^i}{i!} \frac{A_2 + iA_4}{A_2 + iA_4 - k_{\mathrm{agg}}} \mathrm{e}^{-(A_2 + iA_4 + 1/\tau_{\mathrm{M}})t} + \left([\mathrm{Py}^*_{\mathrm{agg}}]_{(t=0)} + [\mathrm{Py}^*_{\mathrm{diff}}]_{(t=0)} \mathrm{e}^{-A_3} \sum \frac{A_3^i}{i!} \frac{A_2 + iA_4}{A_2 + iA_4 - k_{\mathrm{agg}}} \right) \times \mathrm{e}^{-(k_{\mathrm{agg}} + 1/\tau_{\mathrm{M}})t} \quad \text{(B3)}$$

Having an expression for $[\mathrm{Py}^*_{\mathrm{agg}}]_{(t)}$ allows one to calculate $[\mathrm{E1}^*]_{(t)}$ by integrating eq 9d. Summing up the so-obtained expression of $[\mathrm{E1}^*]_{(t)}$ with that of $[\mathrm{E2}^*]_{(t)}$ obtained in eq B2 yields the time-dependent behavior of the excimer $[\mathrm{E}^*]_{(t)}$ given in eq 10b.

References and Notes

(1) Glass, J. E. Hydrophilic Polymers. Performance with Environmental Acceptability *Adv. Chem. Ser.* **1996**, *248*. Schulz, D. N.; Glass, J. E. Polymers as Rheology Modifiers *ACS Symp. Ser.* **1989**, *462*. Glass, J. E. Polymers in Aqueous Media *Adv. Chem. Ser.* **1989**, *223*.

(2) Shay, G.; Bassett, Rex, J. D. *JOCCA* **1993**, UC615.

(3) Tanaka, F.; Edwards, S. F. *Macromolecules* **1992**, *25*, 1516−1523. Semenov, A. N.; Joanny, J.-F.; Khokhlov, A. R. *Macromolecules* **1995**, *28*, 1066−1075. Annabale, T.; Buscall, R.; Ettelaie, R.; Shepherd, P.; Whittlestone, D. *Langmuir* **1994**, *10*, 1060−1070.

(4) Petit-Agneli, F.; Iliopoulos, I. *J. Phys. Chem. B* **1999**, *103*, 4803−4808. Chassenieux, C.; Nicolai, T.; Durand, D.; François, J. *Macromolecules* **1998**, *31*, 4035−4037. Petit, F.; Iliopoulos, J.; Audebert, R. *Polymer* **1998**, *39*, 751−753.

(5) Birks, J. B. *Photophysics of Aromatic Molecules*; Wiley: New York, 1970; pp 301−371.

(6) Covitch, M. J. *SAE Tech Paper* 1999-01-3463.

(7) Sen, A.; Rubin, I. D. *Macromolecules* **1990**, *23*, 2519−2524.

(8) Nemeth, S.; Jao, T.-C.; Fendler, J. H. *Macromolecules* **1994**, *27*, 5449−5456. Jao, T.-C.; Mishra, M. K.; Rubin, I. D.; Duhamel, J.; Winnik, M. A. *J. Polym. Sci., Part B: Polym. Phys.* **1995**, *33*, 1173−1181.

(9) Heinen, W.; Rosemöller, C. H.; Wenzel, C. B.; de Groot, H. J. M.; Lugtenburg, J.; van Druin, M. *Macromolecules* **1996**, *29*, 1151−1157. References in 14.

(10) Winnik, M. A. *Acc. Chem. Res.* **1985**, *18*, 73−79. Winnik, M. A.; Li, X.-B.; Guillet, J. E. *Macromolecules* **1984**, *17*, 699−702.

(11) Mathew, A. K.; Siu, H.; Duhamel, J. *Macromolecules* **1999**, *32*, 7100−7108.

(12) Winnik, F. M. *Chem. Rev.* **1993**, *93*, 587−614.

(13) Lee, S.; Duhamel, J. *Macromolecules* **1998**, *31*, 9193−9200.

(14) (a) Mathew, A. K.; Duhamel, J.; Gao, J. *Macromolecules* **2001**, *34*, 1454−1469.

(15) Char, K.; Frank, C. W.; Gast, A. P. *Macromolecules* **1989**, *22*, 3177−3180.

(16) Tachiya, M. *Chem. Phys. Lett.* **1975**, *33*, 289−292. Infelta, P. P.; Gratzel, M.; Thomas, J. K. *J. Phys. Chem.* **1974**, *78*, 190−195.

(17) Vangani, V.; Duhamel, J.; Nemeth, S.; Jao, C.-T. *Macromolecules* **1999**, *32*, 2845−2854.

(18) Demas, J. N. *Excited-State Lifetime Measurements*; Academic Press: New York, 1983; pp 102−111.

(19) (a) Press: W. H.; Flannery, B. P.; Teukolsky, S. A.; Vetterling, W. T. *Numerical Receipes. The Art of Scientific Computing (Fortran Version)*; Cambridge University Press: Cambridge, 1992; pp 523−528. (b) Press: W. H.; Flannery, B. P.; Teukolsky, S. A.; Vetterling, W. T. *Numerical Receipes. The Art of Scientific Computing (Fortran Version)*; Cambridge University Press: Cambridge, 1992; pp 509−513. (c) Press: W. H.; Flannery, B. P.; Teukolsky, S. A.; Vetterling, W. T. *Numerical Receipes. The Art of Scientific Computing (Fortran Version)*; Cambridge University Press: Cambridge, 1992; p 282.

(20) Duhamel, J.; Yekta, A.; Ni, S.; Khaykin, Y.; Winnik, M. A. *Macromolecules* **1993**, *26*, 6255−6260. Duhamel, J.; Kanyo, J.; Dinter-Gottlieb, G.; Lu, P. *Biochemistry* **1996**, *35*, 16687−16697.

(21) Jones, A.; Dickson,; T. J.; Wilson, B.; Duhamel, J. *Macromolecules* **1999**, *32*, 2956−2961.

(22) Piçara, S.; Gomes, P. T.; Martinho, J. M. G. *Macromolecules* **2000**, *33*, 3947−3950.

(23) Some examples include Principi, T.; Ester Goh, C. C.; Liu, R. C. W.; Winnik, F. M. *Macromolecules* **2000**, *33*, 2958−2966; Mizusaki, M.; Morishima, Y.; Winnik, F. M. *Macromolecules* **1999**, *32*, 4317−4326; Martinho, J. M. G.; Castanheira, E. M. S.; Reis e Sousa, A. T.; Saghbini, S.; André, J. C.; Winnik, M. A. *Macromolecules* **1995**, *28*, 1167−1171; Hu, Y.; Kramer, M. C.; Boudreaux, C. J. McCormick, C. L. *Macromolecules* **1995**, *28*, 7100−7106.